Musa, I, Seabright, AP, Barlow, J and Nishimura, Y

 MuRF1 Partners With TRIM72 to Impair Insulin Signaling in Skeletal Muscle Cells

https://researchonline.ljmu.ac.uk/id/eprint/27256/

Article

For more information please contact researchonline@ljmu.ac.uk

RESEARCH ARTICLE OPEN ACCESS

MuRF1 Partners With TRIM72 to Impair Insulin Signaling in Skeletal Muscle Cells

Ibrahim Musa[1,2] | Alex Peter Seabright[1] | Jonathan Barlow[1,3] | Yusuke Nishimura[1,4]

[1]School of Sport, Exercise and Rehabilitation Sciences, University of Birmingham, UK | [2]Department of Human Physiology, Faculty of Basic Medical Sciences, College of Health Sciences, Prince Abubakar Audu University, Anyigba, Nigeria | [3]Cellular Health and Metabolism Facility, College of Life and Environmental Sciences, University of Birmingham, Birmingham, UK | [4]Research Institute for Sport & Exercise Sciences, Liverpool John Moores University, Liverpool, UK

Correspondence: Ibrahim Musa (ibrophs@yahoo.com) | Yusuke Nishimura (y.nishimura@ljmu.ac.uk)

ABSTRACT

Muscle RING-finger protein 1 (MuRF1, gene name: *TRIM63*) is well known as a critical molecular regulator in skeletal muscle atrophy. Despite the identification of several substrates and interaction partners for MuRF1, the precise molecular mechanisms by which MuRF1 causes skeletal muscle atrophy remain unclear. To gain further insight into the underlying mechanism of skeletal muscle atrophy, we applied targeted biochemical approaches and identified tripartite motif-containing protein 72 (TRIM72) as a novel MuRF1-interacting protein. Subsequent analysis using MuRF1 knockout and rescue experiments showed that TRIM72 protein abundance is dependent on the presence of MuRF1 protein. Furthermore, TRIM72 protein level was increased by dexamethasone treatment in C2C12 myotubes, alongside increased MuRF1 protein level. Dexamethasone decreases IRS1/Akt signaling and glucose uptake specifically in wild type myotubes, but not in MuRF1 KO myotubes. Further analysis showed that overexpression of TRIM72 impairs IRS1/Akt signaling without the presence of MuRF1, indicating that MuRF1 induces a negative impact on insulin signaling through a plausible cooperation with TRIM72. Our findings provide novel non-degradative molecular roles of MuRF1 that link together skeletal muscle atrophy and impaired insulin sensitivity.

1 | Introduction

Muscle RING-finger protein 1 (MuRF1; gene name: *TRIM63*) is a muscle-specific E3 ligase highly critical in skeletal muscle atrophy [1, 2], but how MuRF1 regulates skeletal muscle mass at the molecular level remains poorly understood [1]. MuRF1 protein increases in several human and rodent models of denervation-, immobilization-, or unweighting-induced skeletal

muscle atrophy [1–6]. Consistent with this, MuRF1 gene deletion can partially prevent denervation- and dexamethasone-induced skeletal muscle atrophy in mice [1,2]. Mechanistically, MuRF1 was reported to target myofibrillar proteins, such as myosin heavy chains (MHC), Myosin Binding Protein-C (MyBP-C), Myosin Light Chains 1 (MyLC1), and Myosin Light Chains 2 (MyLC2) for ubiquitylation and subsequent degradation via the ubiquitin proteasome system (UPS) to promote skeletal muscle atrophy [7, 8]. MuRF1 is widely accepted as a biomarker of muscle atrophy, but recent studies suggest that it may also regulate a range of other non-degradative cellular processes [9–11].

Impaired insulin signaling is known as a key driver of muscle protein degradation [12], primarily through reduced Akt activity, which leads to decreased FOXO phosphorylation, thereby increasing the protein abundance of the E3 ubiquitin ligase MuRF1 [13, 14]. However, the molecular links between insulin signaling and MuRF1-dependent muscle atrophy remain unclear. A recent study led by Labeit et al. [15] suggested that MuRF1 overexpression negatively regulates glucose metabolism in diabetic mice by impairing PI3K/Akt signaling. Their study showed that MuRF1 knockout (KO) mice exhibit an increased Akt phosphorylation at Ser473 in skeletal muscle [15]. Interestingly, a treatment of MyoMed-205 stabilizes the serum glucose in the diabetic mice [15]. Similarly, MuRF1 knockout mice revealed that MuRF1 negatively regulates insulin sensitivity [16]. These findings may point to a possible mechanistic link between MuRF1 and insulin signaling, raising the possibility that MuRF1 may play a role in insulin resistance and subsequent muscle wasting [17].

Besides MuRF1, several E3 ligases have been shown to regulate the IRS1/Akt signaling pathway. For example, Cbl-b (Casitas B-lineage lymphoma proto-oncogene-b), another RING-type E3 ligase, catalyzes the ubiquitylation of the IRS1 protein and promotes its degradation in glucocorticoid-induced atrophy [18]. Blocking the interaction between Cbl-b and the IRS1 protein using phosphopentapeptide DGpYMP prevents glucocorticoid-induced atrophy [19]. SCF-Fbxo40 is also another E3 ligase that ubiquitylates and degrades IRS1 upon IGF-1 stimulation [20]. In a previous study, SCF-Fbxo40 was found to be overexpressed in denervation-induced atrophy [21], whereas SCF-Fbxo40 knockdown in mice using siRNA (small-interfering RNA) results in a thicker myotube diameter [20]. TRIM72 (tripartite motif-containing protein 72), another muscle-specific RING-type E3 ligase, ubiquitylates and promotes the degradation of IRS1 in cells [22, 23]. In contrast, TRIM72 knockdown in mice activates Akt and promotes myogenesis [23, 24]. However, these findings are contradicted by Philouze and colleagues, who reported that TRIM72 is not a critical regulator of insulin signaling in their in vitro and in vivo experimental models [25]. This discrepancy may be explained by differences in experimental design, as TRIM72's negative effects on insulin signaling appear to be specific to models of severe diabetes [26]. Supporting this notion, Wu et al. [27] demonstrated that high-glucose and insulin levels, mimicking the diabetic milieu, stimulate the secretion of TRIM72 from muscle tissue. While MuRF1, TRIM72, and Cbl-b E3 ligases have RING domains that facilitate ubiquitin transfer, MuRF1 and TRIM72 also have B-box and coiled-coil

domains that mediate protein–protein interactions [28]. Consistently, MuRF1's B-box2 domain has been shown to interact with muscle-type creatine kinase [11] and titin [29] in skeletal muscle. Surprisingly, a recent study demonstrated that inhibiting MuRF1 reduced both MuRF1 and TRIM72 levels in obese ZSF1 rats [30], indicating a possible functional interaction between these two E3 ligases.

The number of substrates that MuRF1 targets for ubiquitylation is currently unclear, making it difficult to understand how MuRF1 overexpression causes muscle atrophy. A recent study led by Baehr et al. [2] suggests that MuRF1 could induce muscle atrophy via previously unexplored non-degradative mechanisms. In their study, MuRF1 overexpression in mice was sufficient to cause atrophy, but the majority of its ubiquitylated target proteins do not undergo degradation [2]. Further analysis by Baehr et al. [2] showed that MuRF2, MuRF3, and TRIM25 E3 protein abundances were positively correlated with MuRF1 overexpression [2], demonstrating that MuRF1 may coordinate with other E3 ligases to regulate skeletal muscle mass. This highlights the need to explore MuRF1's non-canonical roles and its interactors.

This study examined the molecular function of MuRF1 and its interplay with TRIM72 in skeletal muscle myotubes. To model insulin resistance and atrophy that replicate features of advanced diabetes, we employed dexamethasone treatment, a well-established method validated in rodents and C2C12 cell lines [31–33]. We identified TRIM72 as a novel interacting partner of MuRF1 and validated their association in living cells. Skeletal muscle myotubes lacking MuRF1 showed a significant reduction in TRIM72 protein, while the MuRF1 rescue experiment restored TRIM72 protein abundance. To examine the functional significance of this interaction, we compared wild-type and MuRF1 knockout myotubes under a dexamethasone (Dex) treatment. Dex treatment upregulated both MuRF1 and TRIM72, concomitant with impaired IRS1/Akt signaling and diminished glucose uptake, effects that were absent in MuRF1-deficient cells. These findings establish TRIM72 as a critical effector of MuRF1's role in muscle atrophy and insulin resistance, providing new mechanistic insights into the interplay between proteolytic and metabolic pathways in skeletal muscle.

2 | Materials and Methods

2.1 | Antibodies and Reagents

The following antibodies were applied for western blot analysis: Anti-MuRF1 (Santa Cruz SC-398608; 1:1000), Anti-TRIM72 (Antibodies.com A84884; 1:8000), Anti-phospho Akt (Ser473) (Cell Signaling Technology 4060; 1:1000), Anti-phospho-Akt (T308) (Cell Signaling Technology 2965; 1:1000), Anti-phospho-P70 S6K1 (T389) (Cell Signaling Technology 9234; 1:1000), Anti-GAPDH (Cell Signaling Technology 5174; 1:1000), Anti-IRS1 (Cell Signaling Technology 3407; 1:1000), Anti-GFP (Chromotek 3H9-100; 1:2000), Anti-FLAG M2 (Sigma-Aldrich F1804; 1:1000), Anti-Vinculin (Abcam ab73412; 1:1000), Anti-Myosin (fast) (Sigma M4276; 1:1000), Anti-PAX7 antibody (ThermoFisher; PA1-117, 1:1000), and

Anti-Myosin (Slow) (Sigma M8421; 1:1000). The following secondary HRP-linked antibodies were applied: Anti-goat (Cell Signaling Technology 7077; 1:10000), Anti-mouse (Cell Signaling Technology 7076; 1:10000), Anti-rabbit (Cell Signaling Technology 7074; 1:10000), and Anti-rat (Cell Signaling Technology 7077; 1:5000) antibodies. The reagents for cell culture that were used include: High-glucose GlutaMAX Dulbecco's Modified Eagle Medium with 1 mM of sodium pyruvate (Thermo Fisher Scientific, Loughborough, UK, 31966021); Cytiva hyclone foetal bovine serum (Fisher Scientific, South America, 10 309 133); Penicillin–Streptomycin (10 000 Units/mL–μg/mL); Horse serum (Sigma-Aldrich, Cambridgeshire, UK, H1270); DPBS (Sigma, 14 190); polybrene infection reagent (Merck life scientific UK, TR-1003); and 0.05% phenol red Trypsin–EDTA (Fisher Scientific, 25 300 062); Polyethylenimine (PEI) solution (Sigma, 408 727); Puromycin (Sigma-Aldrich, P8833); GAG/POL and VSV-G plasmids purchased from Clonetech (Saint-Germain-en-Laye, France). Chemicals/compounds such as Dexamethasone (Sigma-Aldrich D4902) and Insulin solution human (Sigma-Aldrich, Poole, UK; I9278) were used.

2.2 | Cell Lines and Culture

L6 rat and C2C12 mouse skeletal muscle myoblasts were purchased from the American Type Culture Collection (ATCC, Manassas, VA, USA). GFP-MuRF1 knocked-in (KI) and MuRF1 knockout (KO) C2C12 cell lines were developed using the CRISPR/Cas9 system as described previously [34].

Firstly, the sense and antisense sgRNA constructs for A (tCT-GATTCCTGATGGAAACGCTA, GCTGATCTGCCCCATCTG CCTtG); sense and antisense sgRNA constructs for B (tCT-GGAGAAGCAGCTGATCTGCC, tGAGATGTTTACCAAG-CCTGTcG), which target the N-terminal GFP knock-in to the MuRF1 locus, and the Nter GFP donor (pMK-RQ vector, DU60520) were generated via the CRISPR vector designing tool (http://tools.genome-engineering.org). The generated oligonucleotides identified were annealed to their respective complements with the cloning tag "a", "g" as was shown in the following: Nter KI as A (TAGCGTTTCCATCAGGAATCAGa, CaAGGCAGATGGGGCAGATCAGC) and Nter KI as B (GGCAGATCAGCTGCTTCTCCAAGa, CgACAGGCTTGGT AAACATCTCa) to generate dsDNA inserts with compatible overhangs to the BbsI restriction site of pBabeD-puro and pX335-Cas9-D10A vectors. The antisense sgRNA was cloned onto pX335-spCas9-D10A (Addgene, 42335) and the sense sgRNA cloned onto the pBabeD-puro (puromycin selectable plasmid P U6). C2C12 myoblasts cells of 60%–70% confluency were co-transfected with 1 μg CRISPR plasmids and 3 μg of the fluorescent GFP tag donor plasmid using polyethylenimine (PEI) transfection reagent. After 48 h co-transfection, the transfected C2C12 mouse skeletal muscle cell was selected using 2 μg/mL puromycin. The selected pool of clones was subsequently single-cell sorted and collected into 96 well plates using the ARIA fusion sorter (BD Biosciences, Berkshire, UK). This was carried out by a specialist at the University of Birmingham's flow cytometry center (Institute of Biomedical Research). Positive clones for GFP-MuRF1 KI and MuRF1 KO C2C12 were validated by immunoblotting.

L6 stably expressing GFP-MuRF1 and GFP empty were generated using a retrovirus encoding human MuRF1 protein fused with a GFP tag at the N-terminus or a retrovirus encoding a GFP empty, respectively. Briefly, cDNA plasmids for a human MuRF1 protein fused with a GFP tag at the N-terminus or a GFP empty were cloned into a pBABED.puro vectors, respectively. The construct was co-transfected into HEK293 FT cells with GAG/POL and VSV-G expression plasmids (Clonetech, Saint-Germain-en-Laye, France) for retrovirus production using polyethylenimine (PEI) transfection reagent in accordance with the manufacturer's instructions. Virus was harvested 48 h after transfection and applied to L6 skeletal muscle myoblasts in the presence of 10 μg/mL polybrene (Sigma-Aldrich, Cambridgeshire, UK). After 48 h of infection, the infected L6 rat skeletal muscle cell was selected using 2 μg/mL puromycin. Positive GFP-MuRF1 and GFP were cultured for further expansion and cryopreserved after being validated by western blotting. All myoblast cells were cultured and grown in high-glucose Dulbecco's modified eagle medium (DMEM) supplemented with 10% (v/v) fetal bovine serum and 1% (v/v) Penicillin–Streptomycin (10000 units/mL–μg/mL). At about 90% confluency, skeletal muscle myoblasts were differentiated into myotubes for at least 5 days using high-glucose DMEM supplemented with 2% (v/v) horse serum (HS) and 1% (v/v) penicillin–streptomycin (10000 units/mL-μg/mL). To maintain cells or myotubes' viability, the medium was changed every 2 days until cells were fully differentiated. The description of drug treatment on myotubes was discussed in the respective figure legends.

2.3 | Transient Transfection of Mammalian Cell Lines

Transient transfections were performed using Polyethylenimine (PEI) transfection reagent. Specifically, maintained culture cells or myotubes were transfected with the required plasmid DNA in a 1:2.5 ratio (μL/μg) of PEI to the plasmid. Briefly, PEI and plasmid DNA were firstly mixed individually in a separate eppendorf tubes containing 500 μL DMEM devoid of serum for 5 min at room temperature. After 5 min of incubation, the PEI/DNA mixture was combined into one and was further incubated for 20 min before being added dropwise onto the cells or myotubes. After overnight incubation, fresh media were replaced to wash out PEI remnants after transfection. At 48 h post transfection, cells were lysed and harvested for analysis.

2.4 | Cell Lysis

At the end of experiments, cells or myotubes prewashed with ice-cold DPBS were lysed and collected in cold sucrose lysis buffer containing 250 mM of sucrose, 10 mM of sodium β-glycerolphosphate, 50 mM of Tris-base (pH 7.5), 5 mM of sodium pyrophosphate, 50 mM of sodium fluoride, 1 mM of EDTA, 1 mM of benzamidine, 1 mM of EGTA, 1 mM of sodium orthovanadate, 1% of Triton X-100, 1× complete Mini EDTA-free protease inhibitor cocktail, and 100 mM of 2-chloroacetamide. Lysates were pelleted for 15 min at 4°C at 13000 rpm, and the supernatant was collected and stored at −80°C for analysis. Protein extracts were quantified with Bradford's assay using BSA as protein standards.

2.5 | Sample Preparation

Protein lysates were prepared using 1× LDS sample buffer (NuPAGE, Invitrogen, NP0008). Samples were left overnight in 1.5% of 2-mercaptoethanol to denature at room temperature before analysis.

2.6 | GFP Pull Down

20 μL of GFP-trap agarose or IgG bead slurry prewashed with an ice-cold DPBS was then washed twice with ice-cold sucrose lysis buffer before being incubated with 2 mg lysates overnight on a rotating wheel at 4°C. Beads were then pelleted by centrifugation at 3500 rpm for 1 min at 4°C. After being pelleted (washing) three times with sucrose lysis buffer, the co-immunoprecipitated proteins were eluted with 2× NuPAGE LDS sample buffer. Samples were left overnight in 1.5% of 2-mercaptoethanol to denature at room temperature before analysis.

2.7 | Western Blotting

Aliquots from the prepared samples were loaded and run on 10% Bis/Tris gels (ThermoFisher Scientific, Leicestershire, UK) in 1× MOPS buffer (ThermoFisher Scientific, Leicestershire, UK) for approximately 75 min at 140 V. Proteins from the gel were transferred to 0.2 μM PVDF (polyvinylidene fluoride) membranes (Millipore, Hertfordshire, UK) in 1× transfer buffer containing 20 mM Tris base, 150 mM glycine, and 20% methanol for 1 h at 100 V and 4°C. The membranes were blocked for 1 h in 5% (w/v) dried skimmed milk diluted with TBS-T (Tris-buffered saline Tween 20): 20 mM of Tris base, P^H, 137 mM of sodium chloride, and 0.1% of Tween-20. To wash off the residual milk solution, membranes were washed three times for 10 min each in TBS-T prior to incubation in primary antibodies prepared in 3% of BSA diluted with TBST. Membranes were incubated in primary antibody on a rocker at 4°C overnight. Membranes were washed three times for 10 min each in TBST before incubating in horseradish peroxidase conjugated secondary antibodies for 1 h at room temperature. After membranes were washed three times for 10 min each in TBST, antibody binding detection was performed using enhanced chemiluminescence (ECL) horseradish peroxidase substrate detection kit (Millipore, Hertfordshire, UK). G: BOX Chemi-XR5 (Syngene, Cambridgeshire, UK) was used to acquire images.

2.8 | Glucose Uptake Measurements

Glucose uptake was measured using "Promega Glucose Uptake Glo assay" as described elsewhere [35]. Briefly, 20 000 cells were seeded into each well of a 96-well plate. At 90% confluence, differentiation was initiated by replacing growth media with 100 μL DMEM supplemented with 2% horse serum. C2C12 WT and MuRF1 KO myotubes pre-treated with 1 μM of dexamethasone (Dex) or 0.1% ethanol (vehicle control) for 24 h were serum-starved overnight before the assay. After overnight serum starvation, wells were washed with 100 μL DPBS and myotubes were incubated with or without 1 μM insulin for 1 h in a 5% CO_2, 95% air incubator at 37°C. After the incubation, myotubes were washed with 100 μL DPBS. Next, 1 mM 2DG in DPBS was added to each well (including myotube-free wells as blank control) for 30 min at 25°C. After which, stop buffer was added to each well to lyse the myotubes, which were then transferred to a 384-well plate and neutralized with Neutralization Buffer. Following a brief shake at 500 rpm, 20 μL of detecting reagent was applied to all wells and kept in the dark for 1 h at 25°C. Luminescence was assessed using a BMG Labtech FLUOstar Omega microplate reader (Aylesbury, UK). Control wells (2DG: without myotubes) provided the assay background and were subtracted from all conditions. Values for glucose uptake are total 2DG accumulation per well, corrected for background (wells without cells), and expressed as fold-change relative to non-insulin-stimulated controls within each genotype/treatment group.

2.9 | Data Analysis

ImageJ/Fiji (National Institutes of Health, USA) was used for protein band quantification. The proteins of interest were normalized in relation to the experimental controls.

2.10 | Statistical Analysis

GraphPad Prism Software version 9 (San Diego, California, USA) was used to run all the statistical analyses. One-way analysis of variance was used for multiple group comparisons. For time course and dose response experiments, one-way analysis of variance was performed before Dunnett's multiple comparisons post hoc test analysis. Two-way analysis of variance of genotype (WT vs. KO) and treatment (Con vs. DEX) was performed before Tukey's multiple comparisons post hoc test analysis. All presented data are mean ± SD. Statistical significance was set at $p < 0.05$. The number of biological replicates and independent experiments performed is described in the figure legends.

3 | Results

3.1 | Identification of TRIM72 as a Novel MuRF1-Interacting Protein

The convergence of TRIM72 and MuRF1, on the negative regulation of insulin signaling and the finding that MuRF1 inhibition decreases TRIM72 prompted us to firstly investigate the interactions between these two proteins. To investigate this, we first generated L6 skeletal muscle cell lines that stably express GFP-MuRF1 or GFP alone, as a control. The generated cells were differentiated into myotubes. Protein lysates were prepared and subjected to GFP pulldown, followed by immunoblotting for TRIM72. Our results showed that TRIM72 co-immunoprecipitated with MuRF1, confirming a direct interaction between these two proteins in cell (Figure 1A, upper panel).

Due to the lack of antibodies that are appropriate for MuRF1 immunoprecipitation, MuRF1 N-terminal GFP knock-in (GFP-MuRF1) C2C12 muscle cells were generated using CRISPR/Cas9
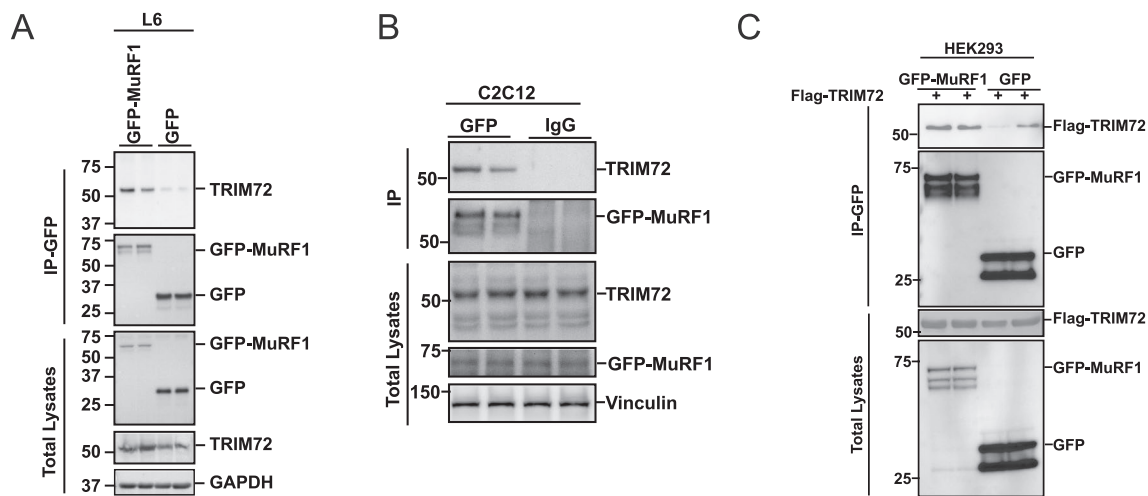
FIGURE 1 | MuRF1 interacts with TRIM72 in skeletal muscle cells. (A) Verification of MuRF1 interaction with endogenous TRIM72 in L6 myotubes that stably expressed GFP-MuRF1. Total lysates (1 mg) from L6 myotubes that stably expressed GFP-MuRF1 or GFP-empty were subjected to GFP pulldown using GFP-Trap agarose beads. The pulldown products were immunoblotted with the indicated antibodies. To confirm protein abundance and loading control, total lysates (lower panel) were immunoblotted with the indicated antibodies. Immunoblots were representative of three independent experiments. (B) Verification of endogenous MuRF1 interaction with endogenous TRIM72 in GFP-MuRF1 knock-in C2C12 myotubes. Total lysates (1 mg) from GFP-MuRF1 knock-in C2C12 myotubes were subjected to GFP pulldown using GFP-Trap agarose beads or beads bound with IgG (as a control). The pulldown products and immunoprecipitates were immunoblotted with the indicated antibodies. To confirm protein abundance and loading control, total lysates (lower panel) were immunoblotted with the indicated antibodies. Immunoblots were representative of three independent experiments. (C) Verification of MuRF1 and TRIM72 interaction in HEK293 cells. HEK293 cells were transiently co-transfected with FLAG-TRIM72 and either with GFP-MuRF1 or GFP-empty (as a control) for 48 h. Total lysates (0.5 mg) were subjected to pulldown using GFP-Trap agarose beads. The pulldown products were immunoblotted with the indicated antibodies. To confirm exogenous protein abundance, total lysates (lower panel) were immunoblotted with the indicated antibodies. Immunoblots were representative of one experiment.

technology to test the interaction between MuRF1 and TRIM72 under endogenous conditions and in a different muscle cell line. The way the KI system is set up via CRISPR/Cas9-mediated insertion of a GFP tag at the N-terminus of the endogenous MuRF1 locus makes it likely that total GFP-MuRF1 levels are similar to WT levels, which means that TRIM72 abundance remains the same as MuRF1 (Figure S1). Again, GFP pulldown showed that TRIM72 co-immunoprecipitated with GFP-MuRF1, but not with IgG (Figure 1B). These results demonstrated that MuRF1 and TRIM72 physically interact also in C2C12 skeletal muscle cells. To further confirm the interaction between MuRF1 and TRIM72 in another cell type, we transiently co-transfected Flag-TRIM72 either with GFP-MuRF1 or GFP-empty in HEK293 cells. The GFP pulldown products were immunoblotted with the Flag-tagged HRP-conjugated antibody for TRIM72. The results showed that TRIM72 was pulled down together with GFP-MuRF1, and its interaction was notably reduced in the GFP-alone control, although with some variability between samples (Figure 1C, upper panel). These results showed that MuRF1 interacts with TRIM72 in different cell types when one or both are overexpressed, explaining why MuRF1 inhibition reduces TRIM72 protein levels in a previous study [30].

3.2 | TRIM72 Protein Abundance Is Dependent on the Presence of MuRF1 Protein in C2C12

We next examined whether TRIM72 constitutes a functional interaction partner or represents a substrate of MuRF1 protein. We used CRISPR/Cas9 technology to generate a MuRF1 knockout (KO) in the C2C12 skeletal muscle cell line. Myoblasts

of wild-type (WT) or two different clones of MuRF1 KO C2C12 were differentiated into myotubes. As expected, MuRF1 protein content was not detected in MuRF1 KO cells, indicating the successful knockout of MuRF1 (Figure 2A). Notably, TRIM72 protein levels were significantly reduced in MuRF1 KO myotubes, compared to WT (Figure 2A,B). Despite the inter-clonal variation, both clones consistently showed TRIM72 reduction vs. WT ($p < 0.0001$; Figure 2B). The difference between Clone 1 and Clone 2 likely reflects inherent clonal variability, which is common in CRISPR-Cas9-generated cell lines due to stochastic genomic or epigenetic heterogeneity [36]. For the benefit of reproducibility, Clone 1 was chosen for the subsequent experiments. We next examined if a transient reintroduction of MuRF1 could restore TRIM72 protein abundance. TRIM72 protein was partially restored when Flag-MuRF1 was transiently overexpressed in the MuRF1 KO cells (Figure 2C,D). It is known from previous studies that these two proteins increase during the differentiation [24, 37]. Thus, the restoration of TRIM72 protein when MuRF1 was added in MuRF1 KO myotubes led us to compare their functional relationship during the differentiation time course (Figure 2E,F). The data showed that TRIM72 protein abundance is associated with MuRF1 upregulation along the differentiation time course, but MuRF1 protein increases first and then TRIM72 protein (Figure 2E,F). Taken together, our results suggest that the abundance of TRIM72 protein is MuRF1 protein upregulation dependent in skeletal muscle cells, demonstrating the contextual functional relationship between TRIM72 and MuRF1 proteins. Previous studies demonstrated that TRIM72 is a known negative regulator of IRS1/Akt signaling [22, 38]. We therefore further explored the roles of MuRF1 and TRIM72 in IRS1/Akt signaling.
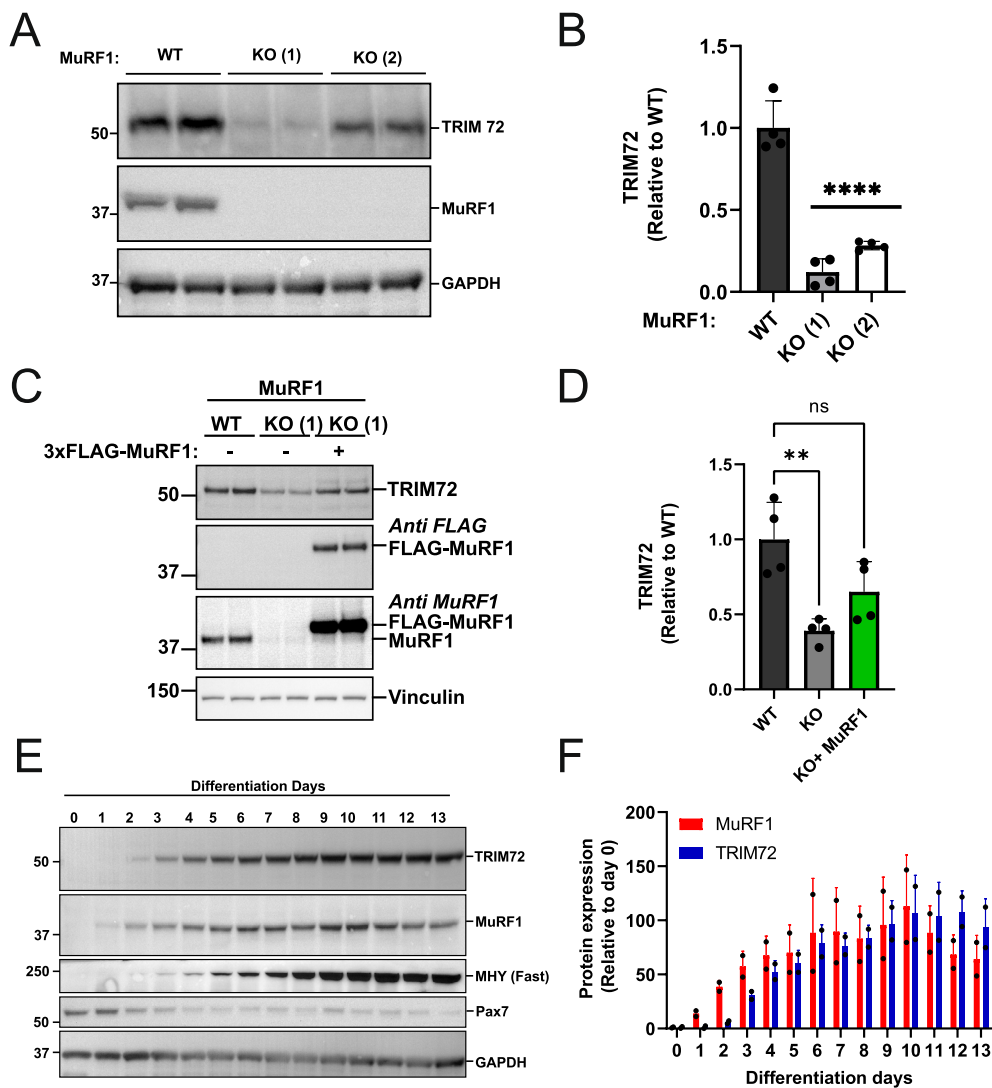
FIGURE 2 | TRIM72 abundance is associated with MuRF1 upregulation in C2C12 myotubes. (A) TRIM72 protein levels are reduced in MuRF1 knockout C2C12 myotubes. Total lysates from WT (wild type) or two different MuRF1 knockout (KO 1 and 2) C2C12 myotubes were analyzed by immunoblotting and probed with the indicated antibodies. Immunoblots were representative of four independent experiments. (B) Quantification of TRIM72 protein abundance in WT and MuRF1 KO C2C12 myotubes. Quantitative data from (A) were normalized to WT and subjected to one-way analysis of variance (ANOVA) before Dunnett's multiple comparisons post hoc test analysis. Error bars indicate the mean ± standard deviation ($n = 4$). ****$p < 0.0001$ compared to WT. (C) Transient overexpression of MuRF1 restored TRIM72 protein abundance in MuRF1 KO myotubes. Total lysates of C2C12 myotubes from WT or MuRF1 KO with and without transient transfection of 3xFLAG-MuRF1 for 48 h were analyzed by immunoblotting and probed with the indicated antibodies. Immunoblots were representative of four independent experiments. (D) Quantification of TRIM72 protein abundance in WT and MuRF1 KO with and without transient transfection of 3xFLAG-MuRF1. Quantitative data from (C) were normalized to WT and subjected to one-way analysis of variance (ANOVA) before Dunnett's multiple comparisons post hoc test analysis. Error bars indicate the mean ± standard deviation ($n = 4$). ****$p < 0.0001$ compared to WT. (E) Representative blots of two independent experiments showing MuRF1 and TRIM72 protein abundance during differentiation time course for up to 13 days in C2C12 cells. Total lysates from C2C12 cells at the indicated days of differentiation were analyzed by immunoblotting and probed with the indicated antibodies. (F) Bar chart analysis of MuRF1 and TRIM72 protein abundance during differentiation time course in C2C12 cells. Quantitative data from (E) were normalized to day 0 and presented as a bar chart. $n = 2$ in each time point.

3.3 | Dexamethasone Increases TRIM72 and MuRF1 Protein Abundances While Decreasing IRS1/Akt Signaling in C2C12 Myotubes

Here we aim to determine the functional relationship between TRIM72 and MuRF1 in relation to insulin signaling impairment using dexamethasone treatment, a well-established method validated in rodents and C2C12 cell lines [31–33, 35]. MuRF1 protein content is known to be increased in

dexamethasone (Dex) treated C2C12 myotubes [39]. We next examined whether TRIM72 protein is similarly upregulated in dexamethasone treated C2C12 myotubes. As expected, Dex treatment increased MuRF1 and also TRIM72 protein abundance (Figure 3B,C). Pearson's correlation coefficient analysis from the Dex dose–response treatment data (Figure 3D) shows a positive correlation between TRIM72 and MuRF1 protein abundance ($r = 0.698$, $p < 0.0001$). Previous studies showed that overexpression of TRIM72 reduces IRS1 protein levels in

C2C12 myotubes [22]. After showing that MuRF1 and TRIM72 proteins are both upregulated after Dex treatment, we wanted to know whether IRS1 protein level is also reduced by Dex treatment. We observed that IRS1 protein level (Figure 3E), Akt phosphorylation at Ser 473 (Figure 3F) and Thr 308 (Figure 3G) were reduced by 1 μM of Dex treatment where

TRIM72 and MuRF1 protein content increased. Additionally, the reduced phosphorylation status in the downstream of mTOR, such as p70 S6K1 phosphorylation at Thr 389, further supported the decreased Akt activity (Figure 3H). Taken together, these results show that MuRF1 and TRIM72 proteins are both upregulated by Dex treatment with a concomitant
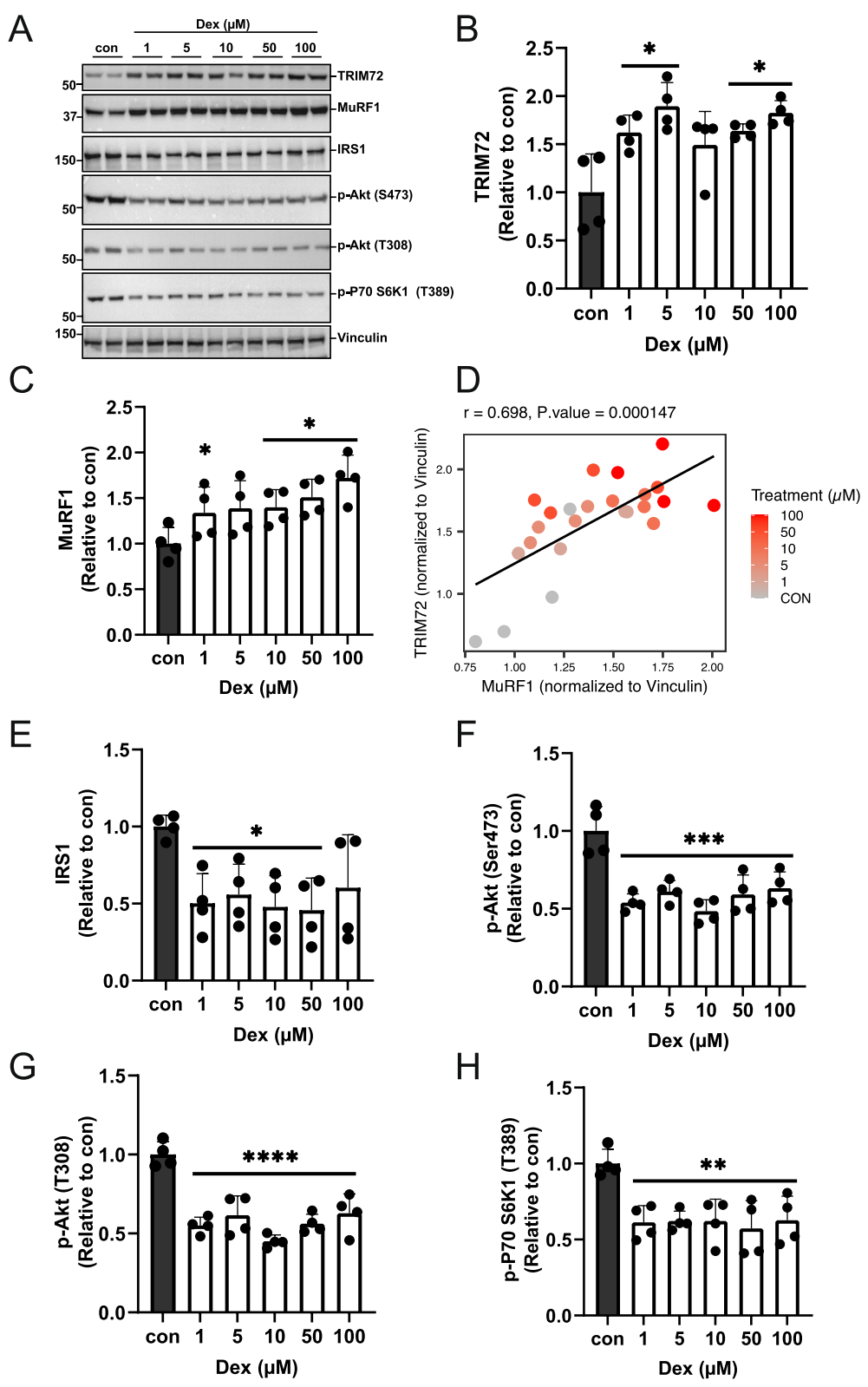

FIGURE 3 | Legend on next page.

FIGURE 3 | Dexamethasone increases TRIM72 and MuRF1 protein abundance while decreasing proximal insulin signaling in C2C12 myotubes. Total lysates from C2C12 myotubes treated with 0.1% ethanol as controls (con) or with indicated concentrations of dexamethasone (Dex) for 24 h were analyzed by immunoblotting and probed with the indicated antibodies. (A) Representative blots showing the effect of dexamethasone on TRIM72, MuRF1 proteins, and proximal insulin signaling in C2C12 myotubes. Immunoblots were representative of four independent experiments. (B, C, E–H) Quantitative data of TRIM72, MuRF1, and IRS1 protein abundances and proximal insulin signaling, including Akt and p70 S6K1 phosphorylation status. Quantitative data were normalized to control (con) and subjected to one-way analysis of variance (ANOVA) before Dunnett's multiple comparisons post hoc test analysis. Error bars indicate the mean ± standard deviation ($n = 4$ independent experiments). Statistical analysis was considered significant at *$p < 0.05$, **$p < 0.01$, ***$p < 0.001$, ****$p < 0.0001$, compared with control. (D) Scatter plot comparing the TRIM72 protein abundance and MuRF1 protein abundance in C2C12 myotubes treated with dexamethasone. Each data point represents data from $n = 4$ independent experiments across 6 treatment groups (total $n = 24$), with color indicating dexamethasone treatment concentration (μM).

reduction of the IRS1/Akt signaling. Based on the effectiveness of the Dex concentrations (Figure 3A,C), 1 μM Dex was chosen for the subsequent experiments.

3.4 | Dexamethasone-Induced Downregulation of Proximal Insulin Signaling and Insulin-Stimulated Glucose Uptake Are Prevented in MuRF1 KO C2C12 Myotubes

MuRF1 knockout cells were used to further confirm whether the TRIM72-mediated downregulation of IRS1/Akt signaling is MuRF1 dependent. The results showed that Dex treatment reduced IRS1 protein levels and Akt phosphorylation at serine 473 in WT, but not in MuRF1 KO myotubes (Figure 4A). These data confirm that MuRF1 protein is required for the TRIM72-mediated downregulation of IRS1/Akt signaling in Dex-treated C2C12 myotubes. To further confirm that MuRF1 is required for Dex-mediated global insulin sensitivity, we measured insulin-stimulated glucose uptake. Dex treatment significantly reduced insulin-stimulated 2-Deoxyglucose (2DG) uptake (Figure 4F) from 1.52 to 0.49-fold difference in WT ($p = 0.0032$), but had no effect in MuRF1 KO myotubes (fold difference; 1.55 in con and 1.35 in DEX, $p = 0.7175$). These results suggest that MuRF1 is required for TRIM72-mediated reduction in IRS1/Akt signaling, which in turn alters insulin-mediated metabolism, including glucose uptake.

3.5 | Restoration of TRIM72 in C2C12 MuRF1 KO Myotubes Decreases Proximal Insulin Signaling

TRIM72 overexpression is known to reduce IRS1 protein levels in C2C12 myotubes [22]. To verify if TRIM72 is an essential intermediary between MuRF1 and Dex-induced reduction in IRS1/Akt signaling, we conducted a rescue experiment by transiently transfecting Flag-TRIM72 into MuRF1 KO myoblasts. As expected, overexpression of TRIM72 in MuRF1 KO significantly reduced IRS1 protein (Figure 5A,B) and phosphorylation of its downstream targets, such as Akt at Ser 473 and p70 S6K1 at Thr 389 (Figure 5). Overall, our data demonstrated that restoration of TRIM72 in MuRF1 KO is sufficient to reduce IRS1 protein and its downstream signaling targets by Dex treatment. This observation indicates that TRIM72 is sufficient to impair IRS1/Akt signaling, but TRIM72 protein is controlled by a MuRF1-dependent manner, highlighting both MuRF1 and TRIM72 as key regulators of IRS1/Akt signaling in skeletal muscle cells.

4 | Discussion

In our study, we discovered TRIM72 as a novel MuRF1 effector protein in skeletal muscle cells. Our findings demonstrated that MuRF1 regulates TRIM72 protein abundance, enabling TRIM72 to downregulate IRS1/Akt signaling and impair insulin-stimulated glucose uptake under dexamethasone treatment in skeletal muscle cells. MuRF1 KO myotubes further confirm the requirement of MuRF1 for the detrimental effects of TRIM72 under dexamethasone treatment though TRIM72 itself is sufficient to impair IRS1/Akt signaling. These results suggest that MuRF1 may regulate muscle mass by acting as a negative regulator of anabolic pathways. Thus, this study provides new evidence that MuRF1 can influence skeletal muscle homeostasis through a non-degradative pathway, highlighting the need for additional exploration of MuRF1's molecular roles.

It is interesting to note that TRIM72 protein abundance was reduced in MuRF1 knockout myotubes (KO) but was restored when MuRF1 was added (Figure 2). This MuRF1 loss- and gain-of-function experiments strongly suggest that TRIM72 is not a substrate for MuRF1-mediated degradation but rather a partner whose abundance is regulated by MuRF1. Consistently, differentiating C2C12 cells start to show the upregulation of MuRF1 proteins before TRIM72 proteins over a 13-day period of differentiation (Figure 2). This data further supports the result from MuRF1 knockout and rescue experiments indicating that TRIM72 protein abundance is dependent on MuRF1 protein. The significant reduction of TRIM72 in MuRF1 KO myotubes and its restoration upon MuRF1 reintroduction (Figure 2A–D) strongly suggests a regulatory relationship beyond mere correlation. In agreement with this, TRIM72 was downregulated in *tibialis anterior* (TA) muscle after MuRF1 inhibitor (MyoMed 205) was administered to obese ZSF1 rats in a previous study [30]. This finding supports our hypothesis that MuRF1 interacts with and modulates TRIM72.

Here we showed that MuRF1 and TRIM72 proteins are both upregulated after Dex treatment. In a common model of skeletal muscle atrophy, dexamethasone (Dex) treatment is well known to cause atrophy in part through increasing MuRF1 levels [7, 10, 18, 39, 40]. For the first time, we showed Dex treatment upregulates TRIM72 protein abundance (Figure 3B). The upregulation of TRIM72 protein in Dex-treated C2C12 myotubes corresponded with a dramatic decrease in IRS1 protein levels, corroborating previous findings that TRIM72 facilitates IRS1 degradation [22]. Several studies have reported that TRIM72
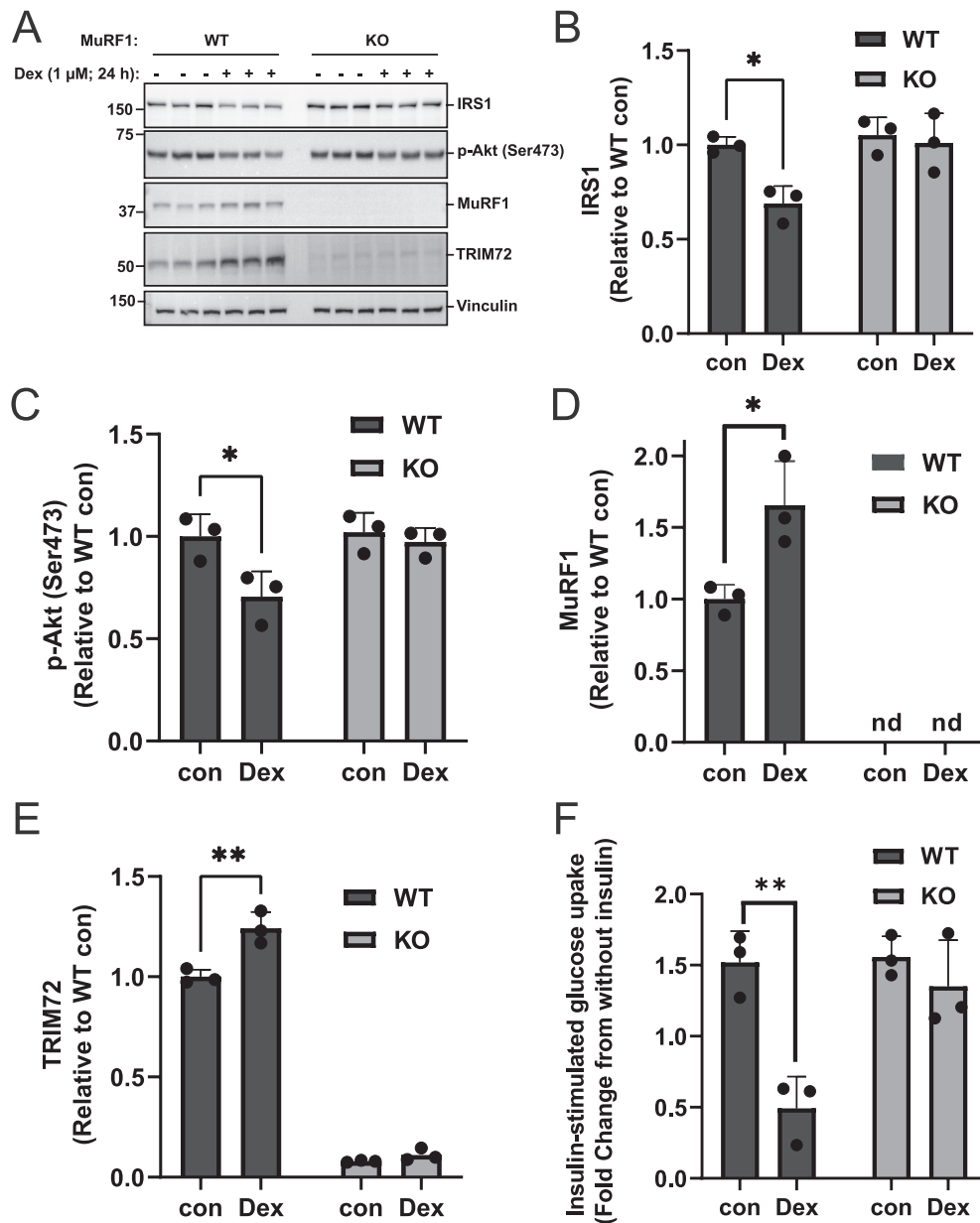
FIGURE 4 | MuRF1 KO prevents dexamethasone-induced downregulation of proximal insulin signaling and insulin-stimulated glucose uptake in C2C12. (A) Immunoblots from three independent experiments showing IRS1, p-Akt (Ser473), MuRF1, and TRIM72 in WT and MuRF1 KO C2C12 myotubes treated with and without dexamethasone. Total lysates from WT or MuRF1 KO C2C12 myotubes treated with and without 1 μM dexamethasone (Dex) for 24 h were analyzed by immunoblotting before probing with the appropriate antibodies. (B–E) Figures showing quantitative data of IRS1 protein abundance (B), Akt Ser473 phosphorylation (C), MuRF1 (D), and TRIM72 (E) protein abundances. Quantitative data from (A) were normalized to wild-type control (WT con) and subjected to a two-way ANOVA before Tukey's multiple comparisons post hoc test analysis. Error bars indicate the mean ± standard deviation ($n = 3$). *$p < 0.05$, **$p < 0.01$, compared to WT con. nd: Non-detectable. (F) Insulin-stimulated 2-Deoxyglucose (2DG) uptake in WT and MuRF1 KO treated with or without dexamethasone. C2C12 WT and MuRF1 KO myotubes pre-treated with or without 1 μM dexamethasone for 24 h were serum-starved overnight, stimulated by 1 μM insulin for 1 h before measuring 2DG uptake for 30 min. Results were presented as glucose uptake (2DG fold-changes) relative to external controls (without insulin stimulation). Data were analyzed by a two-way ANOVA before Tukey's multiple comparisons post hoc test analysis. Error bars indicate the mean ± standard deviation ($n = 3$ independent experiments). **$p < 0.01$ compared with insulin-stimulated control.

ubiquitylates and degrades IRS1 [22–24] via the 26S proteasome, leading to impaired IRS1 signaling (Figure 3). Likewise, MuRF1 knockout mice revealed that MuRF1 can negatively regulate insulin sensitivity [16], underscoring the shared function of these E3 ligases in inhibiting insulin signaling to promote muscle atrophy. This is consistent with a previous study that IRS1 deficiency promotes muscle atrophy both in vivo and in vitro [41, 42]. Thus,

our data provide a potential mechanistic link between muscle wasting and insulin resistance in skeletal muscle.

A reduction in IRS-1 levels is considered a major contributor to the development of catabolic diseases including diabetes [43]. Previous studies with MuRF1 knockout mice revealed that MuRF1 can negatively regulate insulin sensitivity [16], raising
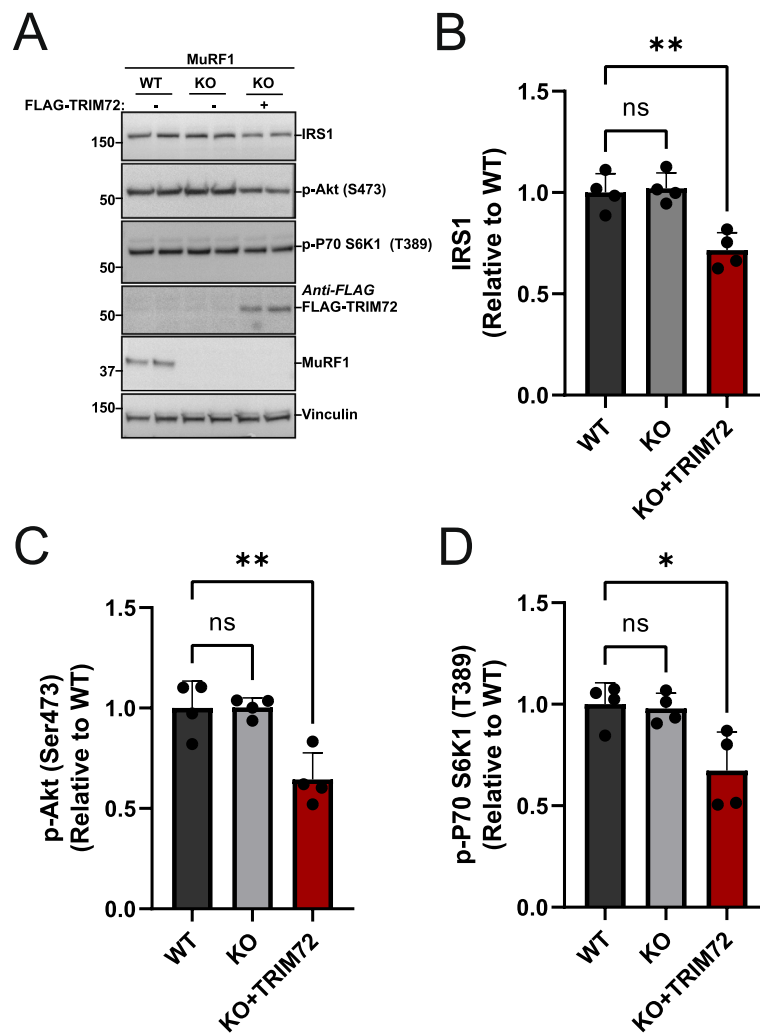
FIGURE 5 | Restoration of TRIM72 in C2C12 MuRF1 KO myotubes decreases proximal insulin signaling. (A) Immunoblots from four independent experiments showing IRS1, p-Akt (Ser473), p70 S6K1 (T389), TRIM72, and MuRF1 in WT and MuRF1 KO C2C12 myotubes. Total lysates of C2C12 myotubes from WT or MuRF1 KO with and without transient transfection of FLAG-TRIM72 for 48 h were analyzed by immunoblotting and probed with the appropriate antibodies. (B–D) Figures showing quantitative data of IRS1 protein abundance (B), Akt Ser (473) phosphorylation (C), and p70 S6K1 (T389) phosphorylation (D). Quantitative data from (A) were normalized to wild-type (WT) and subjected to a one-way ANOVA before Dunnett's multiple comparisons post hoc test analysis. Error bars indicating: Mean ± standard deviation ($n = 4$ independent experiments). $*p < 0.05$, $**p < 0.01$, compared to Wild Type. ns, Non-significant.

the possibility that MuRF1 may be responsible for the insulin resistance linked to muscle wasting [17]. Our findings show that MuRF1 and its interaction partner, TRIM72, negatively affect IRS1/Akt signaling after dexamethasone treatment, corroborating previous studies. In skeletal muscle, TRIM72 functions as an autonomous ubiquitin ligase to degrade the IRS1 protein as a negative regulator of insulin signaling [22–24]. The restored insulin signaling activity in MuRF1 KO C2C12 myotubes (Figure 4A) could be attributed to the marked loss of TRIM72 in the MuRF1 KO C2C12 myotubes. Collectively, our findings support a model wherein the MuRF1-TRIM72 axis acts as a critical negative regulator of insulin signaling in muscle wasting.

Glucose metabolism is essential for maintaining organ function in humans [44]. Dex treatment significantly reduced insulin-induced glucose uptake in WT but not MuRF1 KO myotubes when compared with controls (Figure 4F). Recently, Labeit et al. [15] examined the effect of MuRF1 on glucose

metabolism in diabetic mice. They found diabetic mice exhibit impaired PI3K/Akt signaling, but MuRF1 KO mice exhibit increased Akt phosphorylation at Ser473 in skeletal muscle [15]. Consistently, MuRF1 inhibitor (MyoMed-205) was shown to stabilize serum glucose concentration in diabetic mice [15]. Our results align with previous studies in rodents [22, 26, 27] indicating that TRIM72 is sufficient to promote diabetes through IRS1 downregulation, a finding supported by human data showing elevated TRIM72 and blood glucose following oral glucose administration [27]. However, a contrasting role of TRIM72 in the regulation of diabetes has also been reported [25, 45]. These studies showed that neither the injection of recombinant human TRIM72 (rhTRIM72) nor the adenoviral transfer of the human TRIM72 gene was able to cause changes in blood glucose in either diabetic db/db or nondiabetic mice [25, 45]. This discrepancy may be explained by differences in experimental design, as TRIM72's negative effects on insulin signaling appear to be specific to models of severe diabetes where it exacerbates, rather

than initiates, metabolic dysfunction [26]. In the study by Feng et al. [26], all the db/db mice had fasting blood glucose greater than 10 mmol/L and fed blood glucose greater than 20 mmol/L at 10 weeks of age. Whereas, in the other mouse studies, the average fasting blood glucose was 7 mmol/L and the average fed blood glucose was 13.9 mmol/L at 18–32 weeks of age [25, 45]. These results suggest the need to study these E3 ligases in context-specific disease models of diabetes. Using perfused mouse muscle, Wu et al. [27] showed that high-glucose (25 mmol/L) and insulin levels, conditions mimicking obesity and T2D, induce TRIM72 protein release by muscle [27]. Notably, a previous study by Reddy et al. [46] demonstrated a co-upregulation of MuRF1 and TRIM72 mRNA in a streptozotocin-induced diabetic rat muscle, suggesting that their mutual expression can be regulated at the gene level in a metabolic disease model. Thus, the use of appropriate disease models (highly hyperglycaemic) to accurately model the human condition should be considered for future study to reveal the full role of targets like MuRF1 and TRIM72.

5 | Conclusion

Our study identifies the MuRF1-TRIM72 axis as a crucial regulatory mechanism in dexamethasone-induced metabolic dysfunction. Our findings suggest that insulin-stimulated glucose uptake in skeletal muscle is impaired by a MuRF1-dependent regulation of TRIM72 protein levels. This finding reveals a previously unknown function of MuRF1 in non-proteolytic metabolic regulation and offers a new perspective on the molecular mechanism underlying insulin resistance and muscle atrophy. We propose a mechanistic model wherein the upregulation of MuRF1 raises the levels of TRIM72 protein, which in turn impairs insulin-stimulated glucose uptake in muscle.

Author Contributions

Ibrahim Musa: conceptualization, methodology, validation, visualization, investigation, formal analysis, writing – original draft preparation, reviewing and editing. Alex P. Seabright: formal analysis, writing – reviewing and editing. Jonathan Barlow: methodology, validation, writing – reviewing and editing. Yusuke Nishimura: validation, visualization, formal analysis, writing – reviewing and editing.

Data Availability Statement

The data presented in this study is available on request from the corresponding author.

References

1. S. C. Bodine, E. Latres, S. Baumhueter, et al., "Identification of Ubiquitin Ligases Required for Skeletal Muscle Atrophy," *Science* 294 (2001): 1704–1708.

2. L. M. Baehr, D. C. Hughes, S. A. Lynch, et al., "Identification of the MuRF1 Skeletal Muscle Ubiquitylome Through Quantitative Proteomics," *Function (Oxford, England)* 2 (2021): zqab029.

3. D. Attaix, S. Ventadour, A. Codran, D. Béchet, D. Taillandier, and L. Combaret, "The Ubiquitin–Proteasome System and Skeletal Muscle Wasting," *Essays in Biochemistry* 41 (2005): 173–186.

4. S. H. Lecker, R. T. Jagoe, A. Gilbert, et al., "Multiple Types of Skeletal Muscle Atrophy Involve a Common Program of Changes in Gene Expression," *FASEB Journal* 18 (2004): 39–51.

5. A. J. Murton, D. Constantin, and P. L. Greenhaff, "The Involvement of the Ubiquitin Proteasome System in Human Skeletal Muscle Remodelling and Atrophy," *Biochimica et Biophysica Acta* 1782 (2008): 730–743.

6. D. Taillandier and C. Polge, "Skeletal Muscle Atrogenes: From Rodent Models to Human Pathologies," *Biochimie* 166 (2019): 251–269.

7. B. A. Clarke, D. Drujan, M. S. Willis, et al., "The E3 Ligase MuRF1 Degrades Myosin Heavy Chain Protein in Dexamethasone-Treated Skeletal Muscle," *Cell Metabolism* 6 (2007): 376–385.

8. S. Cohen, J. J. Brault, S. P. Gygi, et al., "During Muscle Atrophy, Thick, but Not Thin, Filament Components Are Degraded by MuRF1-Dependent Ubiquitylation," *Journal of Cell Biology* 185 (2009): 1083–1095.

9. C. C. Witt, S. H. Witt, S. Lerche, D. Labeit, W. Back, and S. Labeit, "Cooperative Control of Striated Muscle Mass and Metabolism by MuRF1 and MuRF2," *EMBO Journal* 27 (2008): 350–360.

10. L. M. Baehr, J. D. Furlow, and S. C. Bodine, "Muscle Sparing in Muscle RING Finger 1 Null Mice: Response to Synthetic Glucocorticoids," *Journal of Physiology* 589 (2011): 4759–4776.

11. S. Koyama, S. Hata, C. C. Witt, et al., "Muscle RING-Finger Protein-1 (MuRF1) as a Connector of Muscle Energy Metabolism and Protein Synthesis," *Journal of Molecular Biology* 376 (2008): 1224–1236.

12. X. Wang, Z. Hu, J. Hu, J. Du, and W. E. Mitch, "Insulin Resistance Accelerates Muscle Protein Degradation: Activation of the Ubiquitin-Proteasome Pathway by Defects in Muscle Cell Signaling," *Endocrinology* 147 (2006): 4160–4168.

13. P. J. Atherton, P. L. Greenhaff, S. M. Phillips, S. C. Bodine, C. M. Adams, and C. H. Lang, "Control of Skeletal Muscle Atrophy in Response to Disuse: Clinical/Preclinical Contentions and Fallacies of Evidence," *American Journal of Physiology. Endocrinology and Metabolism* 311 (2016): E594–E604.

14. Y. Nishimura, J. Chunthorng-Orn, S. Lord, et al., "Ubiquitin E3 Ligase Atrogin-1 Protein Is Regulated via the Rapamycin-Sensitive mTOR-S6K1 Signaling Pathway in C2C12 Muscle Cells," *American Journal of Physiology. Cell Physiology* 323 (2022): C215–c225.

15. S. Labeit, S. Hirner, J. Bogomolovas, et al., "Regulation of Glucose Metabolism by MuRF1 and Treatment of Myopathy in Diabetic Mice With Small Molecules Targeting MuRF1," *International Journal of Molecular Sciences* 22 (2021): 2225.

16. S. Hirner, C. Krohne, A. Schuster, et al., "MuRF1-Dependent Regulation of Systemic Carbohydrate Metabolism as Revealed From Transgenic Mouse Studies," *Journal of Molecular Biology* 379 (2008): 666–677.

17. H. Crossland, S. Skirrow, Z. A. Puthucheary, D. Constantin-Teodosiu, and P. L. Greenhaff, "The Impact of Immobilisation and Inflammation on the Regulation of Muscle Mass and Insulin Resistance: Different Routes to Similar End-Points," *Journal of Physiology* 597 (2019): 1259–1270.

18. R. Nakao, K. Hirasaka, J. Goto, et al., "Ubiquitin Ligase Cbl-b Is a Negative Regulator for Insulin-Like Growth Factor 1 Signaling During Muscle Atrophy Caused by Unloading," *Molecular and Cellular Biology* 29 (2009): 4798–4811.

19. A. Ochi, T. Abe, R. Nakao, et al., "N-Myristoylated Ubiquitin Ligase Cbl-b Inhibitor Prevents on Glucocorticoid-Induced Atrophy in Mouse Skeletal Muscle," *Archives of Biochemistry and Biophysics* 570 (2015): 23–31.

20. J. Shi, L. Luo, J. Eash, C. Ibebunjo, and D. J. Glass, "The SCF-Fbxo40 Complex Induces IRS1 Ubiquitination in Skeletal Muscle, Limiting IGF1 Signaling," *Developmental Cell* 21 (2011): 835–847.

21. J. Ye, Y. Zhang, J. Xu, Q. Zhang, and D. Zhu, "FBXO40, a Gene Encoding a Novel Muscle-Specific F-Box Protein, Is Upregulated in Denervation-Related Muscle Atrophy," *Gene* 404 (2007): 53–60.

22. R. Song, W. Peng, Y. Zhang, et al., "Central Role of E3 Ubiquitin Ligase MG53 in Insulin Resistance and Metabolic Disorders," *Nature* 494 (2013): 375–379.

23. J.-S. Yi, J. S. Park, Y.-M. Ham, et al., "MG53-Induced IRS-1 Ubiquitination Negatively Regulates Skeletal Myogenesis and Insulin Signalling," *Nature Communications* 4 (2013): 2354.

24. C. S. Lee, J. S. Yi, S. Y. Jung, et al., "TRIM72 Negatively Regulates Myogenesis via Targeting Insulin Receptor Substrate-1," *Cell Death and Differentiation* 17 (2010): 1254–1265.

25. C. Philouze, S. Turban, B. Cremers, et al., "MG53 Is Not a Critical Regulator of Insulin Signaling Pathway in Skeletal Muscle," *PLoS One* 16 (2021): e0245179.

26. H. Feng, H. Shen, M. J. Robeson, et al., "MG53 E3 Ligase-Dead Mutant Protects Diabetic Hearts From Acute Ischemic/Reperfusion Injury and Ameliorates Diet-Induced Cardiometabolic Damage," *Diabetes* 71 (2022): 298–314.

27. H.-K. Wu, Y. Zhang, C.-M. Cao, et al., "Glucose-Sensitive Myokine/Cardiokine MG53 Regulates Systemic Insulin Response and Metabolic Homeostasis," *Circulation* 139 (2019): 901–914.

28. K. L. B. Borden, "RING Fingers and B-Boxes: Zinc-Binding Protein–Protein Interaction Domains," *Biochemistry and Cell Biology* 76 (1998): 8.

29. T. Centner, J. Yano, E. Kimura, et al., "Identification of Muscle Specific Ring Finger Proteins as Potential Regulators of the Titin Kinase Domain," *Journal of Molecular Biology* 306 (2001): 717–726.

30. V. Adams, A. Schauer, A. Augstein, et al., "Targeting MuRF1 by Small Molecules in a HFpEF Rat Model Improves Myocardial Diastolic Function and Skeletal Muscle Contractility," *Journal of Cachexia, Sarcopenia and Muscle* 13 (2022): 1565–1581.

31. M. Shalam, M. Harish, and S. Farhana, "Prevention of Dexamethasone-and Fructose-Induced Insulin Resistance in Rats by SH-01D, a Herbal Preparation," *Indian Journal of Pharmacology* 38 (2006): 419–422.

32. K. J. Ragland, K. B. Travis, E. R. Spry, T. Zaman, P. M. Lundin, and R. A. Vaughan, "The Effect of Dexamethasone-Mediated Atrophy on Mitochondrial Function and BCAA Metabolism During Insulin Resistance in C2C12 Myotubes," *Metabolites* 15 (2025): 322.

33. C. Y. Wong, H. Al-Salami, and C. R. Dass, "C2C12 Cell Model: Its Role in Understanding of Insulin Resistance at the Molecular Level and Pharmaceutical Development at the Preclinical Stage," *Journal of Pharmacy and Pharmacology* 72 (2020): 1667–1693.

34. F. A. Ran, P. D. Hsu, J. Wright, V. Agarwala, D. A. Scott, and F. Zhang, "Genome Engineering Using the CRISPR-Cas9 System," *Nature Protocols* 8 (2013): 2281–2308.

35. N. Yamamoto, T. Sato, K. Kawasaki, S. Murosaki, and Y. Yamamoto, "A Nonradioisotope, Enzymatic Assay for 2-Deoxyglucose Uptake in L6 Skeletal Muscle Cells Cultured in a 96-Well Microplate," *Analytical Biochemistry* 351 (2006): 139–145.

36. C. J. Giuliano, A. Lin, V. Girish, and J. M. Sheltzer, "Generating Single Cell–Derived Knockout Clones in Mammalian Cells With CRISPR/Cas9," *Current Protocols in Molecular Biology* 128 (2019): e100.

37. S. Perera, B. Mankoo, and M. Gautel, "Developmental Regulation of MURF E3 Ubiquitin Ligases in Skeletal Muscle," *Journal of Muscle Research and Cell Motility* 33 (2012): 107–122.

38. H. Lee, J. J. Park, N. Nguyen, et al., "MG53-IRS-1 (Mitsugumin 53-Insulin Receptor Substrate-1) Interaction Disruptor Sensitizes Insulin Signaling in Skeletal Muscle," *Journal of Biological Chemistry* 291 (2016): 26627–26635.

39. H. Eo, C. H. Reed, and R. J. Valentine, "Imoxin Prevents Dexamethasone-Induced Promotion of Muscle-Specific E3 Ubiquitin Ligases and Stimulates Anabolic Signaling in C2C12 Myotubes," *Biomedicine & Pharmacotherapy* 128 (2020): 110238.

40. P. Bonaldo and M. Sandri, "Cellular and Molecular Mechanisms of Muscle Atrophy," *Disease Models & Mechanisms* 6 (2013): 25–39.

41. H. Tamemoto, T. Kadowaki, K. Tobe, et al., "Insulin Resistance and Growth Retardation in Mice Lacking Insulin Receptor Substrate-1," *Nature* 372 (1994): 182–186.

42. E. Araki, M. A. Lipes, M. E. Patti, et al., "Alternative Pathway of Insulin Signalling in Mice With Targeted Disruption of the IRS-1 Gene," *Nature* 372 (1994): 186–190.

43. J. L. Bailey, B. Zheng, Z. Hu, S. R. Price, and W. E. Mitch, "Chronic Kidney Disease Causes Defects in Signaling Through the Insulin Receptor Substrate/Phosphatidylinositol 3-Kinase/Akt Pathway: Implications for Muscle Atrophy," *J Am Soc Nephrol* 17 (2006): 1388–1394.

44. H. Du, Y. Zhao, Z. Yin, D. W. Wang, and C. Chen, "The Role of miR-320 in Glucose and Lipid Metabolism Disorder-Associated Diseases," *International Journal of Biological Sciences* 17 (2021): 402–416.

45. Q. Wang, Z. Bian, Q. Jiang, et al., "MG53 Does Not Manifest the Development of Diabetes in Db/Db Mice," *Diabetes* 69 (2020): 1052–1064.

46. S. S. Reddy, K. Shruthi, Y. K. Prabhakar, G. Sailaja, and G. B. Reddy, "Implication of Altered Ubiquitin-Proteasome System and ER Stress in the Muscle Atrophy of Diabetic Rats," *Archives of Biochemistry and Biophysics* 639 (2018): 16–25.

Supporting Information

Additional supporting information can be found online in the Supporting Information section. **Figure S1:** fsb271084-sup-0001-FigureS1.docx.